Title
ESTIMATION OF POWER-ENERGY PLOTS FOR SECONDARY BATTERIES

Authors
McLarnon, F.R.
Cairns, E.J.
Landgrebe, A.R.

Publication Date
1988-05-01

LBL-25253 c.2

Lawrence Berkeley Laboratory
UNIVERSITY OF CALIFORNIA

APPLIED SCIENCE DIVISION

Presented at the 33rd International Power Sources Symposium, Cherry Hill, NJ, June 13–16, 1988

Estimation of Power-Energy Plots for Secondary Batteries

F.R. McLarnon, E.J. Cairns, and A.R. Landgrebe

May 1988

APPLIED SCIENCE DIVISION

Prepared for the U.S. Department of Energy under Contract Number DE-AC03-76SF00098.

LBL-25253

ESTIMATION OF POWER-ENERGY PLOTS FOR SECONDARY BATTERIES

by

Frank R. McLarnon and Elton J. Cairns
Applied Science Division
Lawrence Berkeley Laboratory
University of California
Berkeley, California 94720

and

Albert R. Landgrebe
Office of Energy Storage and Distribution
U.S. Department of Energy
Washington, D.C. 20585

for

33rd International Power Sources Symposium

Cherry Hill, New Jersey

June 13-16, 1988

This work was supported by the Assistant Secretary for Conservation and Renewable Energy, Office of Energy Storage and Distribution of the U.S. Department of Energy under Contract No. DE-AC03-76SF00098.

ESTIMATION OF POWER-ENERGY PLOTS FOR SECONDARY BATTERIES

Frank R. McLarnon and Elton J. Cairns

Applied Science Division
Lawrence Berkeley Laboratory
Berkeley, California 94720

and

Albert R. Landgrebe

Office of Energy Storage and Distribution
U.S. Department of Energy
Washington, D.C. 20585

Energy storage devices are being developed for a wide range of consumer, military and industrial applications. These devices exhibit a number of attractive features, including flexibility in the choice of primary fuel, minimal environmental impact, and rapid deployment. Recent R&D has focused on secondary batteries, primary batteries, fuel cells, capacitors, flywheels, thermal energy storage, magnetic energy storage and chemical energy storage. These technologies have been evaluated on the basis of their performance, cost and durability characteristics, and the selection of a particular technology depends strongly on the requirements of the specific application. Secondary batteries are considered to be leading candidates for a number of energy storage applications, including electric vehicles, stationary electric energy storage (utilities, industry, remote stand-alone), portable consumer and military devices, and aerospace technology.

A plot of a galvanic cell's specific power (W/kg) versus its delivered specific energy (Wh/kg) offers a convenient means to assess the cell's performance. Such plots are particularly valuable when the intended application requires that the cell exhibit both high power *and* energy. These plots were first used in the 1960's (1) to compare the potential of various secondary batteries to provide electric vehicles with acceptable acceleration and range, and they are now routinely used to characterize advanced batteries under development by DOE for such applications (2-8). These plots, which are commonly referred to as Ragone plots, can be generated in a straightforward manner by measuring the discharge capacity of a cell as a function of the discharge power level, provided that the cell and necessary electrical control and measurement equipment are available. However, in many cases the galvanic cell of interest has not yet been developed to point where realistic testing can be performed, so it is necessary to *estimate* the cell's power-energy characteristics.

Estimating Power-Energy Plots

A very simple method to estimate a galvanic cell's power-energy plot follows:

1. **Determine the cell's voltage-capacity behavior.**

   A typical cell's voltage-capacity behavior during constant-current discharge is sketched in Fig. 1. The cell's delivered energy is the area under the curve in such a plot, and it is seen that both the cell's voltage and delivered energy tend to decrease with increasing discharge current. This behavior is the result of a number of contributing factors, including ohmic, kinetic, mass-transfer, material-utilization, thermal, chemical, and physical effects, and it can change dramatically during a single discharge and/or as the cell ages. A greatly simplified cell voltage-capacity plot is shown in Fig. 2. The dashed lines at $V = V_o$ and $Q = Q_o$ represent typical cell behavior at very low discharge currents, where the maximum average cell voltage and capacity are expected. In the absence of any experimental data, V_o can be estimated from tabulated electromotive force data,* and Q_o can be estimated by assuming that there is 100% Faradaic utilization of active material. The presence of parasitic reactions (e.g., gas evolution) will lower Q_o, and it should be noted that complete active-material utilization is rarely attained.

2. **Determine the cell's voltage-current behavior.**

   The slope of a plot of cell voltage vs current is the negative of the cell's effective resistance R. If such data are not available, a rough estimate can be made using the electrolyte conductivity and the cell geometry to calculate the ohmic potential drop in the electrolyte phase, which often dominates the cell's impedance behavior.

3. **Generate a power-energy plot.**

   Based on the idealized voltage-capacity behavior illustrated by the dashed lines in Fig. 2, and making the assumption that the cell's behavior is pseudo-ohmic, the cell's voltage and power are given by:

$$V = V_o - IR \qquad (1)$$

---

* If these are not available, one can divide the change in Gibbs free energy (products-reactants) by [-nF].

and

$$P = IV = I\,(V_o - IR) \qquad (2).$$

Assuming that the cell capacity decreases linearly with increasing current, and that the maximum cell current corresponds to a pseudo-ohmic potential drop equal to V_o, the cell energy is given by:

$$E = VQ = (V_o - IR)\,Q_o\,(1 - \frac{IR}{V_o}) \qquad (3),$$

or

$$\frac{E}{V_o Q_o} = (1 - \frac{IR}{V_o})^2 \qquad (4).$$

By eliminating the cell current I, a power-energy relationship is obtained:

$$P = \frac{V_o^2}{R}\left[\sqrt{\frac{E}{V_o Q_o}} - \frac{E}{V_o Q_o}\right] \qquad (5).$$

The final estimated power-energy plots require that the cell's power and energy be divided by the cell mass, which includes the active material, current collectors, inert electrolyte, cell container, bus bars, insulation and any other necessary peripheral equipment. A useful rule-of-thumb for estimating the attainable specific energy for *rechargeable* cells at the 4-5 hour discharge rate is:

20-25% of theoretical for cells with solid electrodes
15-18% of theoretical for cells with one gas electrode and one solid electrode
14-17% of theoretical for cells with one liquid electrode and one solid electrode.

For *primary* cells, it is possible to achieve up to about 40% of the theoretical specific energy at low discharge rates (10-20 hours).

The form of Eq. 5 shows that the ratio V_o^2/R is an important parameter for estimating peak specific power of a galvanic cell, as well as the shape of its power-energy plot. Gibbard (9), Corrigan (10), and Attia and Rowlette (11) used this parameter (or a similar expression) to characterize the power performance of secondary batteries.

Comparison to Experimental Data

Power-energy plots have been determined for a number of advanced batteries. In particular, high-performance rechargeable batteries, under development for electric vehicle applications, have been extensively characterized. Argonne National Laboratory has published much of this data, and recent attention has been focused on the secondary batteries listed in Table 1.

Table 1. Secondary Battery Characteristics

Battery Couple	Characteristics	
	Theoretical Specific Energy Wh/kg	V_o volts
Pb/PbO_2	175	2.10
Fe/NiOOH	267	1.35
Zn/NiOOH	326	1.74
Zn/Br_2	430	1.85
Na/S	758	2.08

Power-energy data for the electrochemical couples listed in Table 1 were collected. The nominal battery (or module) voltage was used for the value of V_o, which may not correspond to the value V_o shown in Fig. 2, or the value listed in Table 1. The reported battery mass m was used to convert battery power P and battery energy E into specific power $p = P/m$ and specific energy $e = E/m$, respectively.

Figure 3 shows plots of battery specific power p vs specific energy e for different rechargeable batteries. The solid curves represent the power-energy performance predicted by Eq. 5 using Q_o and R as adjustable parameters, and the points are experimental data from the corresponding references listed in Table 2. Equation 5 appears to successfully correlate the experimental power-energy plots for the four rechargeable batteries shown in Fig. 3. The derived (i.e., those used to generate the solid curves in Fig. 3) values of effective battery resistance R and maximum capacity Q_o are listed in Table 2, along with the reported values of battery resistance and nominal capacity. There is reasonable agreement between the derived and nominal values; the nominal capacities are less than the derived maximum capacities, and the derived (pseudo)resistances are generally greater than the measured resistances, as expected.

Table 2. Derived and Experimental Parameters for Power-Energy Plots

Battery Couple	Developer	Ref.	m (kg)	Q_o (Ah) nom.	Q_o (Ah) der.	R (mΩ) expt.	R (mΩ) der.
Pb/PbO_2	Johnson Controls (EV-2300)	2,6,12	57.9	183	200	4.0±0.5	10
Pb/PbO_2*	Johnson Controls (EV-3000)	2,6,12	74.8	249	285	4.0±0.5	12
Fe/NiOOH*	Eagle Picher	2,4,6	36.8	280	300	3.6±0.2	2
Zn/NiOOH*	General Motors	2	17.9	144	152	-	2
Zn/NiOOH	Gould	2,5,13	27.0	225	230	0.7±0.2	3
Zn/Br_2*	Exxon	7	547.3	123	135	-	300
Na/S*	Chloride Silent Power	8	0.12	-	10	-	34
Na/S	Ford Aerospace and Communications	2,3	0.98	55	65	9.0±3.0	8

* The data and curves shown in Figs. 3 and 4 correspond to the batteries marked with an asterisk.

The derived power-energy plot for the Exxon Zn/Br_2 battery is compared to experimental data in Fig. 4. The fit is less satisfactory than those shown in Fig. 3, which may reflect the possibility that the assumptions used to derive Eq. 5 may not hold, over a wide range of power and energy levels, for this flow battery. For example, the Br_2 electrode exhibits greater kinetic polarization (i.e., a non-ohmic effect) at high current densities than do the other electrodes used in these secondary batteries.

Conclusions

The simple method presented here offers a fast and convenient method for estimating power-energy plots for galvanic cells. Comparisons between various electrochemical couples can be made, different cell designs can be evaluated, and parameters such as sustained peak power can be estimated.

Acknowledgement

This work was supported by the Assistant Secretary for Conservation and Renewable Energy, Office of Energy Storage and Distribution of the U.S. Department of Energy.

REFERENCES

1. *The Automobile and Air Pollution: A Program for Progress, Part II*, pp. 49-88, U.S. Department of Commerce (1967).

2. *National Battery Test Laboratory Battery Performance Summary Notebook*, Argonne National Laboratory.

3. "Sodium-Sulfur Battery Development. Phase VB Final Report for the Period October 1, 1981 Through February 28, 1985," Ford Aerospace and Communications Corporation, Final Report for DOE Contract No. DE-AM04-79CH10012 (October 1985).

4. W.H. DeLuca, R.L. Biwer and A.F. Tummillo, "Effects of Operating Temperature on the Characteristics of Nickel/Iron Traction Batteries," Argonne National Laboratory Report No. ANL-86-6 (July 1986).

5. "Annual Report for 1980 on Research, Development, and Demonstration of Nickel-Zinc Batteries for Electric Vehicle Propulsion," Gould Inc. Final Report for DOE Contact No. 31-109-38-4200 (March 1981).

6. W.H. DeLuca, A.F. Tummillo, T.L. Biwer, C.C. Christianson, F. Hornstra and N.P. Yao, "Comparative Response of Lead-Acid and Nickel/Iron Batteries to Pulsed and Constant-Current Loads," Paper No. 8301 presented at the Electric Vehicle Council EXPO '83, Detroit, MI (1983).

7. T.P. Mulcahey, A.F. Tummillo, R.F. Hogrefe, C.C. Christianson, J.F. Miller, J.A. Smaga, J.J. Marr, C.E. Webster and J. Lee, "Zinc/Bromine Battery Evaluations at Argonne National Laboratory," Extended Abstracts: Eighth Battery and Electrochemical Contractors' Conference, Vienna, VA, pp. 122-125 (1987).

8. T.P. Mulcahey, A.F. Tummillo, R.F. Hogrefe, C.C. Christianson, R. Biwer, C.E. Webster, J. Lee, J.F. Miller, J.J. Marr and J.A. Smaga, "Sodium-Sulfur Technology Evaluation at Argonne National Laboratory," Extended Abstracts: Eighth Battery and Electrochemical Contractors' Conference, Vienna, VA, pp. 85-88 (1987).

9. H.F. Gibbard, "Ultra-High-Power Batteries," Proc. Symp. on Electrochemical and Thermal Modeling of Battery, Fuel Cell and Photoenergy Conversion Systems, J.R. Selman and H. Maru, eds., Proc. Vol. 86-12, The Electrochemical Society, Inc., Pennington, NJ, pp. 193-205 (1986).

10. D.A. Corrigan, *J. Power Sources* 21, 33 (1987).

11. A.I. Attia and J.J. Rowlette, "Development of New Sealed Bipolar Lead-Acid Battery," Proc. Space Electrochemical Research and Technology Conference, April 1987, NASA Conference Publication 2484 (1987).

12. Mr. Donáld E. Bowman, private communication (1986).

13. Mr. Geoffrey Barlow, private communication (1986).

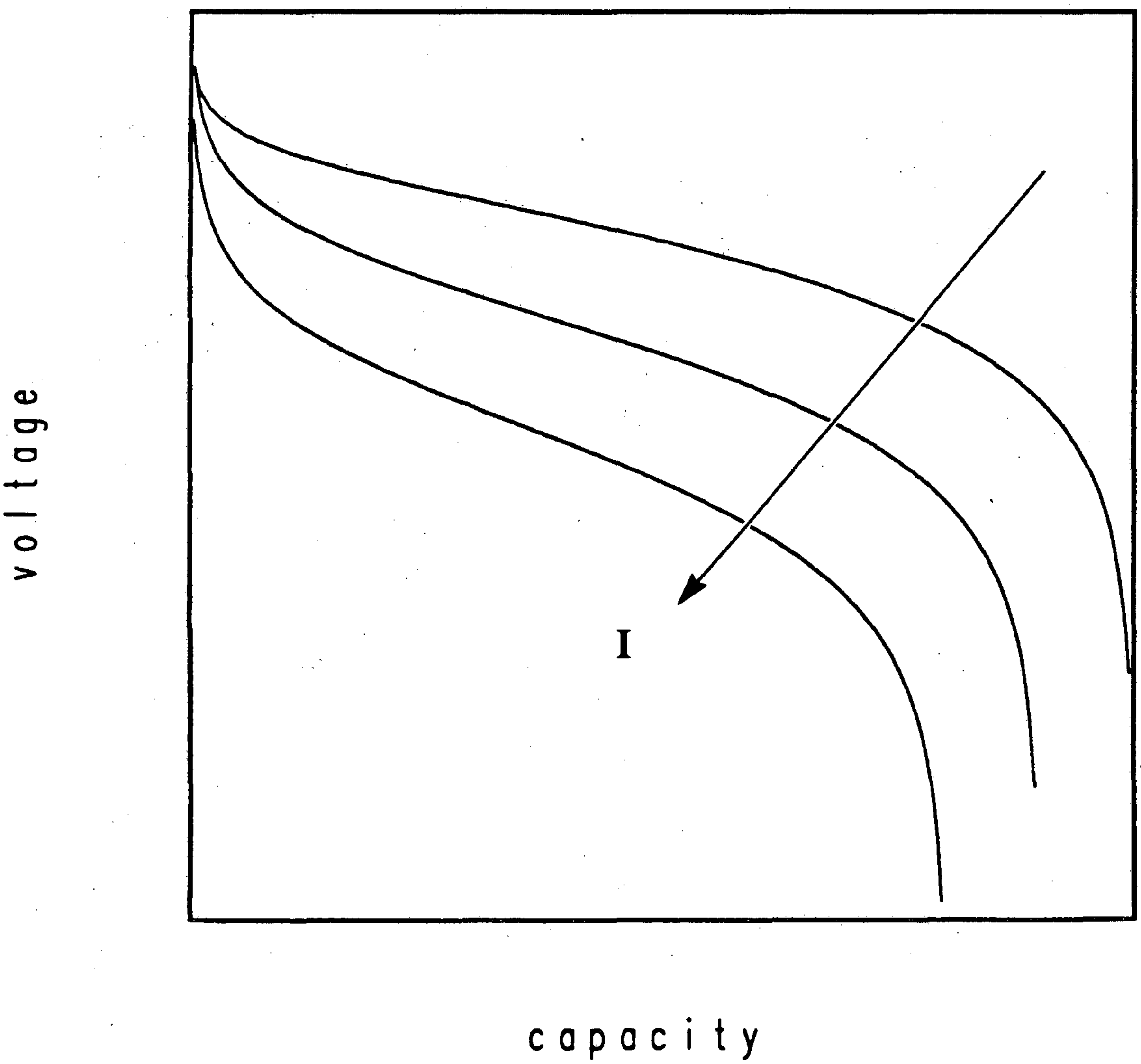

Figure 1. Typical cell voltage-capacity behavior for different cell currents.

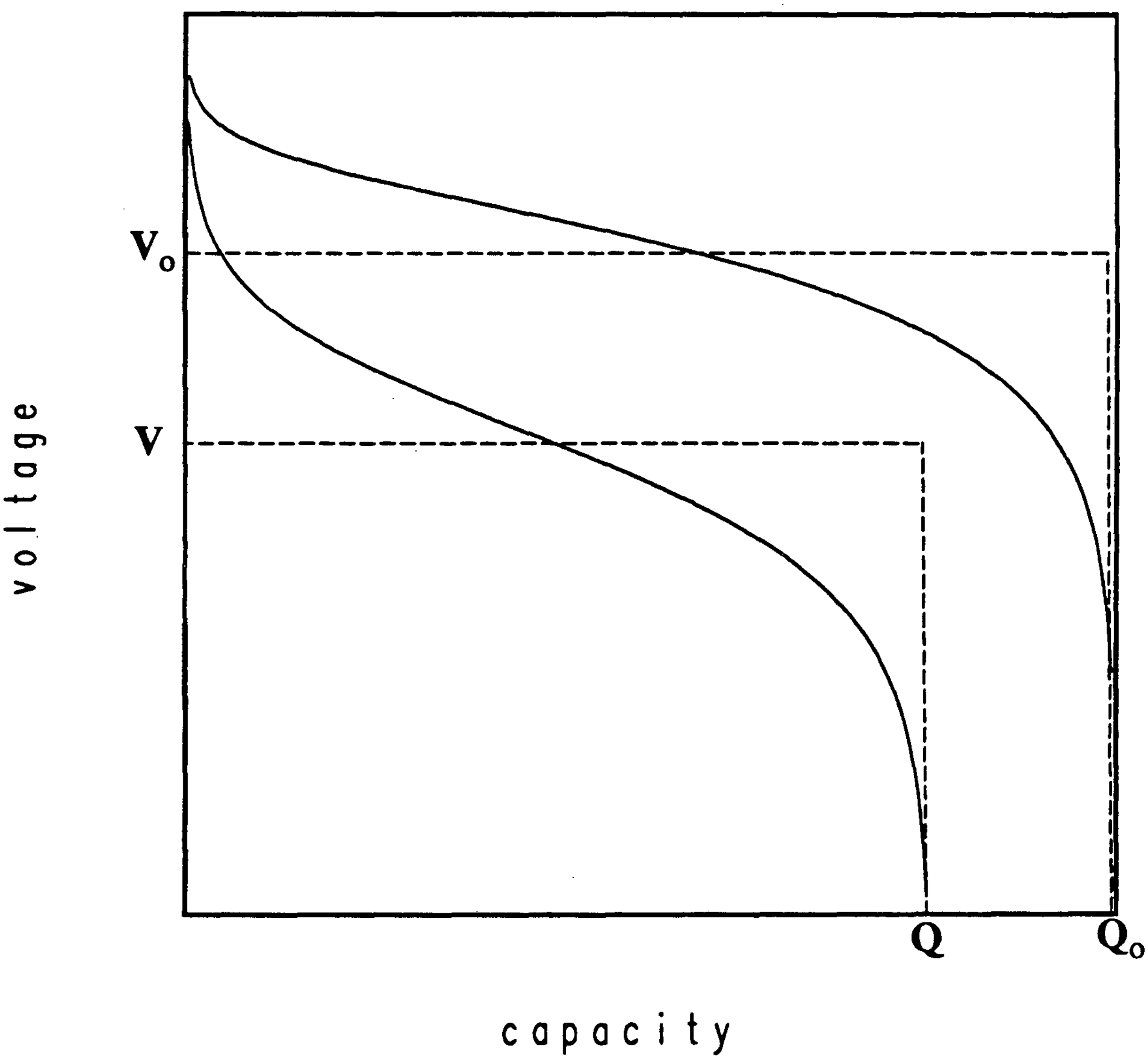

Figure 2. Cell voltage-capacity behavior.
___________ typical data
__ __ __ idealized behavior

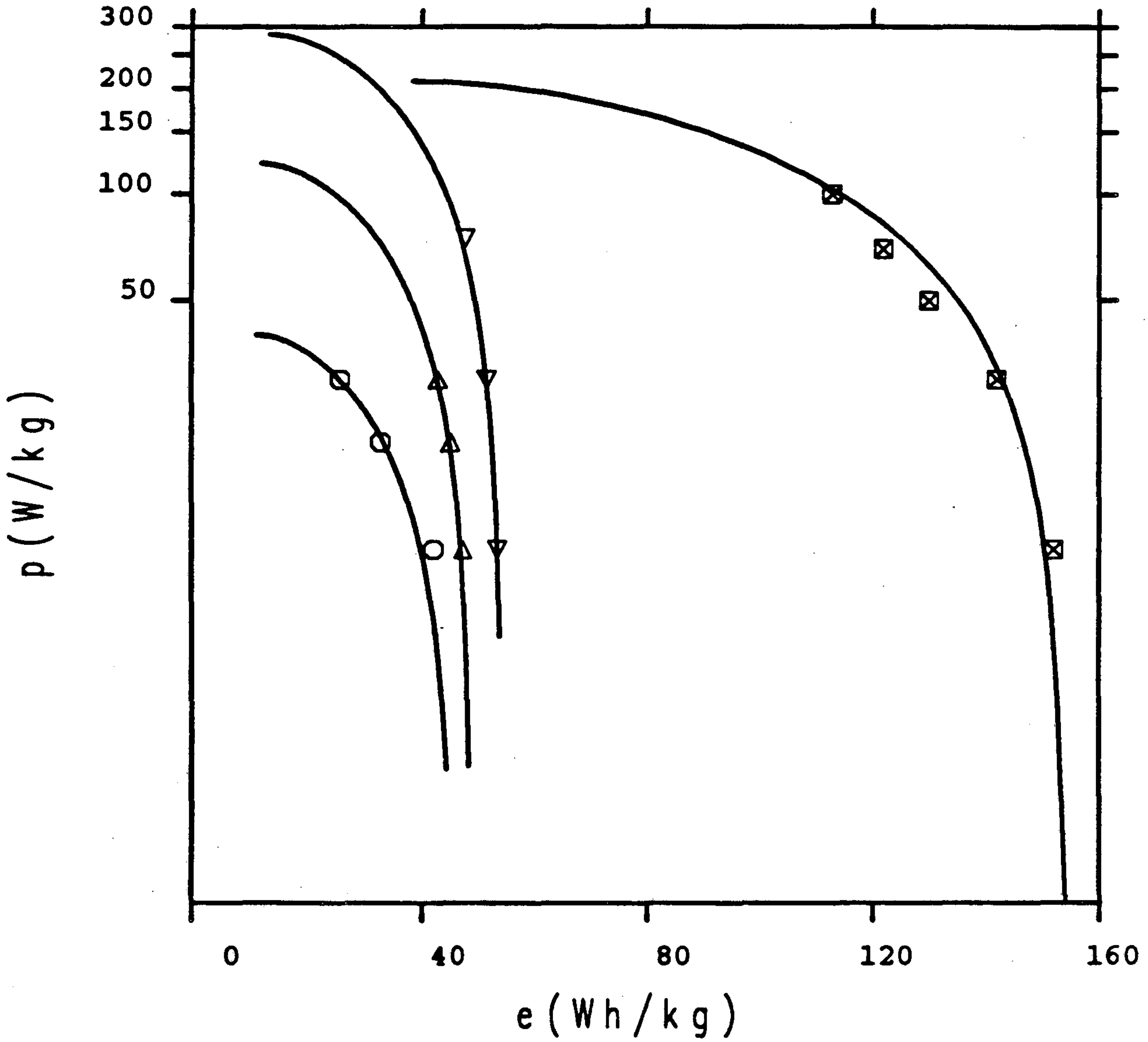

Figure 3. Power-energy plot for various secondary batteries.

——————— Eq. (5), parameters as listed in Table 2

Experimental data from references listed in Table 2

○ $Pb/PbO_2, V_o = 12.0V$
△ Fe/NiOOH, $V_o = 6.0V$
▽ Zn/NiOOH, $V_o = 6.4V$
⊠ Na/S, $V_o = 1.85V$

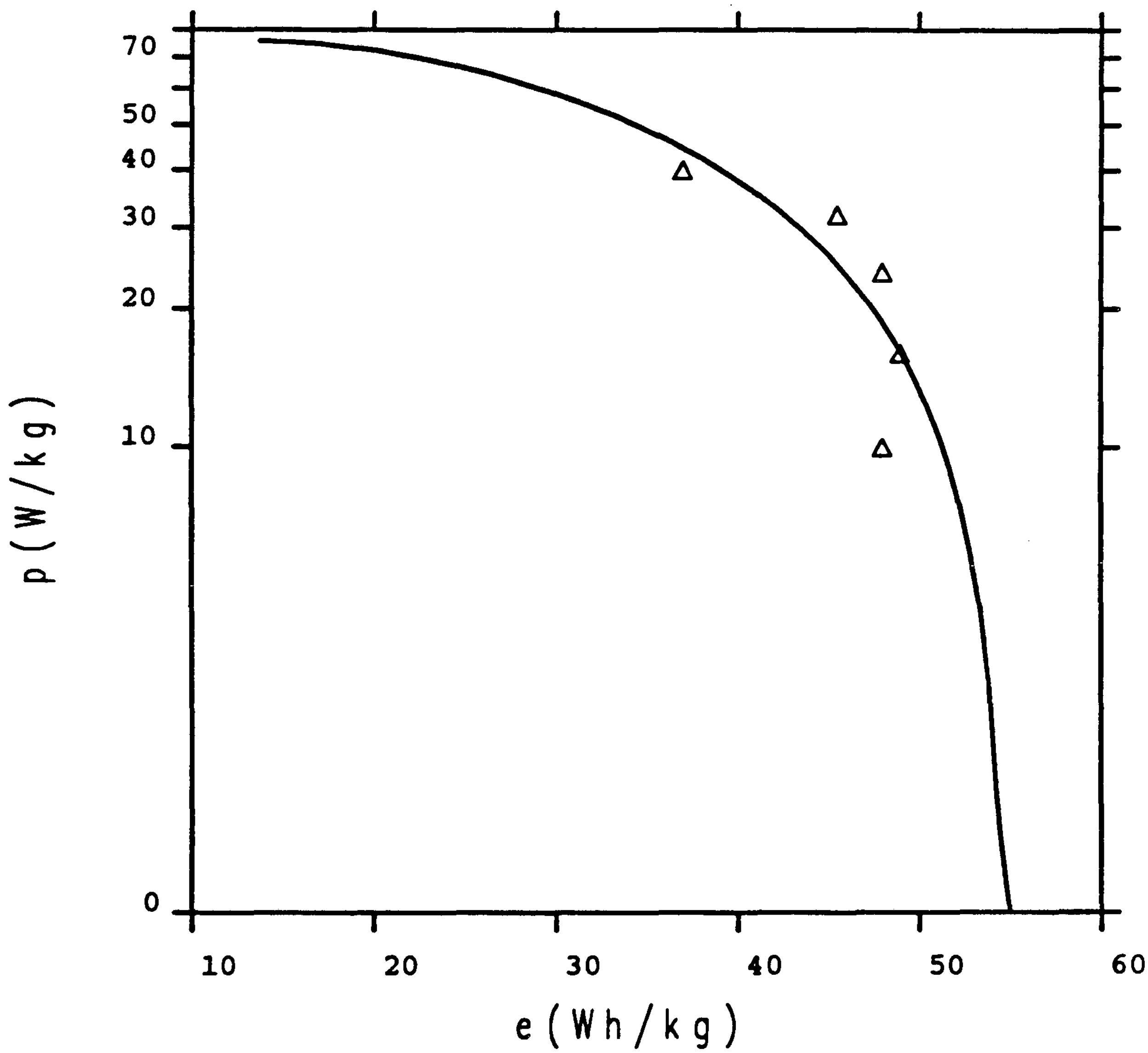

Figure 4. Power-energy plot for a Zn/Br_2 battery.

________ Eq. (5), parameters as listed in Table 2, V_o = 223V

Δ Experimental data from reference (7)